ANL-HEP-CP-97-54

THE ARGONNE WAKEFIELD ACCELERATOR: DIAGNOSTICS AND BEAM CHARACTERIZATION

M. Conde, W. Gai, R. Konecny, X. Li, J. Power, P. Schoessow
Argonne National Laboratory, Argonne, IL 60439, USA
and N. Barov
UCLA, Los Angeles, CA 90024, USA

Abstract

The Argonne Wakefield Accelerator is comprised of two L-band photocathode RF guns and standing wave linac structures. The high charge bunches (20 - 100 nC) produced by the main gun (drive gun) allow us to study the generation of wakefields in dielectric lined structures and plasmas. The secondary gun (witness gun) generates low charge bunches (80 - 300 pC) that are used to probe the wakefields excited by the drive bunches. We use insertable phosphor screens for beam position monitoring. Beam intensity is measured with Faraday cups and integrating current transformers. Quartz or aerogel Cerenkov radiators are used in conjunction with a Hamamatsu streak-camera for bunch length measurements. The beam emittance is measured with a pepper-pot plate and also by quadrupole scan techniques. We present a description of the various diagnostics and the results of the measurements. These measurements are of particular interest for the high current (drive) linac, which operates in a much higher charge regime than other photoinjector-based linacs.

1 EXPERIMENTAL SETUP

The Argonne Wakefield Accelerator (AWA) group operates two photocathode-based RF guns. One of them was designed to produce electron bunches of very high charge (up to 100 nC) and short bunch length (25 – 50 ps FWHM). The high intensity beam from this gun is used to excite wakefields in dielectric-loaded waveguides and also in pre-formed plasma columns. For this reason this gun is referred to as the "drive gun" (which generates the drive beam). The second RF gun generates electron bunches of lower charge (typically 300 pC) that are used to probe the wakefields generated by the drive beam. This gun is then appropriately called the "witness gun".

Figure 1 shows a schematic of the experimental setup [1]. The half-cell drive gun was designed to have a high accelerating field (92 MV/m at the photocathode surface) to allow the extraction of high charge bunches, and to produce a 2 MeV beam with the limited RF power available at the design time (1.5 MW at 1.3 GHz). Magnesium was chosen for the photocathode material for its ruggedness and quantum efficiency (5×10^{-4} The 2 MeV bunches generated by the drive gun subs quently go through two standing-wave, $\pi/2$ mode lin tanks, increasing the beam energy to about 14 MeV. Tl beam is then focused by quadrupoles and bent by thr dipoles to allow for the injection of both the drive bea... and the witness beam into the wakefield experimental section. The witness gun [2] is a 6-cell standing-wave $\pi/2$ mode structure that generates 4 MeV bunches of 300 pC. Its photocathode material is presently copper, but a change to magnesium will occur soon. The witness beam goes through combining optics and then through the dielectric-loaded structure trailing the drive beam, thereby probing the wakefields excited by the drive bunches. Energy changes of the witness beam are measured by a spectrometer located downstream of the wakefield experimental section.

The two RF guns and the two linac structures are powered by a single klystron (Thomson TH2022D; 20 MW, 4 μs pulses), via necessary power spliters and phase shifters. The laser system is comprised of a dye oscillator (496 nm) pumped by a tripled YAG, which is then followed by a dye amplifier, a doubling crystal and finally an excimer amplifier. We thus obtain laser pulses of up to 8 mJ with 6 ps FWHM at 248 nm. The laser beam is then split and a small fraction of it (~ 15%) sent to the witness gun. There is an adjustable delay between the drive gun and the witness gun laser beams. This allows us to vary the delay between the drive and the witness electron bunches (obviously the RF phases have to be adjusted accordingly, in order to maintain the same launching phase).

The AWA control software was developed in house and is based on the Tcl/Tk scripting language. At the core of the control system is an HP-750 RISC workstation which is interfaced to VMEbus. The 68060 CPU board on the VMEbus handles command requests from the workstation and provides auxiliary processing capabilities. Most of the control and monitoring functions are handled through a VME-CAMAC parallel bus interface. VME boards are used to acquire images and oscilloscope traces.

Submitted to the proceedings of the 1997 Particle Accelerator Conference, Vancouver, BC, May 12-16, 1997.

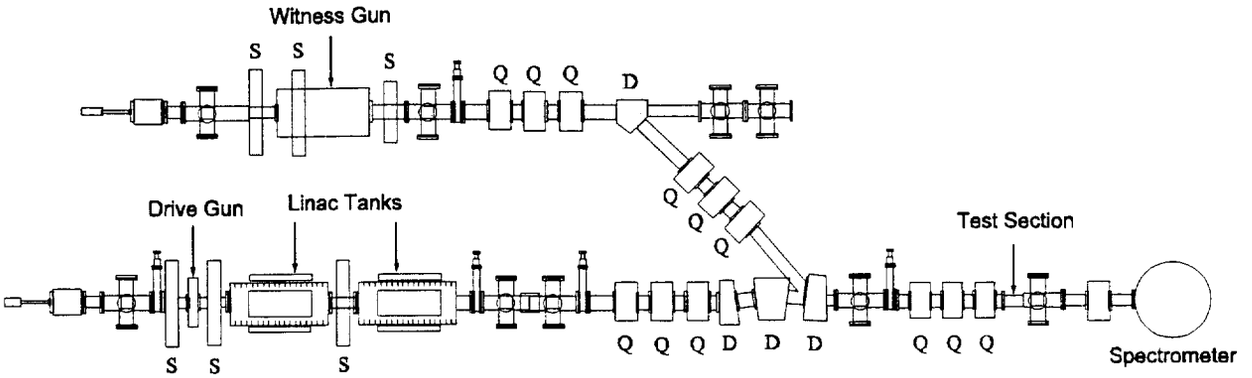

Figure 1: Schematic of the AWA experimental setup; S, Q, and D indicate solenoids, quadrupoles and dipoles, respectively.

2 DIAGNOSTICS

There are four integrating current transformers (Bergoz ICT - 082-070-20:1) installed on the beamlines to measure bunch charge at various locations. Alternatively, we can use insertable Faraday-cups at diagnostic ports along the beamlines and also at the beam-dumps. The ICTs appear to be more reliable, since they are easier to calibrate, while the Faraday-cups suffer from secondary electron emission and electric breakdown due to the high peak voltages generated.

Cerenkov light generated by the electron beams is sent to a Hamamatsu M1952/C1587 streak camera for bunch length measurements. Insertable quartz or aerogel plates are used as Cerenkov radiators. The aerogels require a more elaborate holder, but offer several advantages over the quartz plates. The aerogels need to be in a vacuum-tight holder which is inserted in the beam path. The electron beam enters our holder through a thin aluminum window (0.15 mm). It then traverses the aerogel (under atmospheric pressure) and emits Cerenkov radiation, which leaves the aerogel holder through a quartz window. Our aerogels [3] have an index of refraction of 1.009, therefore the Cerenkov light is emitted at an angle of 7.4° with respect to the direction of propagation of the 14 MeV electrons. The light is then reflected by a mirror and leaves the vacuum chamber through a diagnostic view port.

Contrary to the aerogels, quartz plates are compatible with the vacuum of the accelerator and can be easily inserted in the beam path. However, due to their higher index of refraction (1.54), their Cerenkov light is emitted at an angle of 49.5°, making it difficult to collect more than a small fraction of the total cone of radiation. Multiple reflections within the quartz plate are also a problem to be considered. They can be minimized by placing the plate such that the radially polarized Cerenkov light leaves the plate at the Brewster angle. In practice, because emission in quartz occurs at large angles, it is harder to achieve good alignment of the associated optics to transport the light to the streak camera.

A pepper-pot plate is used for emittance measurements. It consists of a 1.5 mm thick tungsten plate with 0.3 mm diameter holes spaced by 3 mm. A phosphor screen 75 cm downstream of the pepper-pot plate is used to image the resulting beamlets.

3 EXPERIMENTAL RESULTS

We have measured the bunch length of the drive beam as a function of the RF launching phase, for several values of the laser beam energy. By varying the laser energy we change the amount of charge emitted by the photocathode, and thus the influence of the space-charge force in the dynamics of the electron bunches. Figure 2 shows RF phase scans for two different laser beam energies. In these plots the relative RF phase between the drive gun and the linac tanks was kept constant, and only the phase of the klystron power with respect to the laser pulses was changed. The plots show how the bunch length and the extracted charge vary as a function of the launching RF phase. We notice that the dependencies on the RF phase are stronger in the higher charge case, since in that case the space-charge forces are stronger and it becomes more critical to optimize the RF fields. It is also important to optimize the focusing solenoidal fields, otherwise the bunch length may become much longer and even show a bimodal temporal distribution of charge.

Figure 3 shows bunch length as a function of bunch charge. In this plot the RF phases have been set to their optimum values. We have plotted the 95% RMS value of the bunch lengths and also the corresponding FWHM. The ratio between the 95% RMS and the FWHM values shows that the pulses are not gaussian. The large fluctuation in the FWHM of the pulses also shows that the detailed shape of the temporal profile

varies considerably from pulse to pulse. In Fig. 3, the data points represented by circles correspond to the optimum points observed in five RF phase scans (two of which are shown on Fig. 2). The points represented by squares and triangles were measured when the input RF power into the drive gun was at a higher level. We notice that the points represented by the triangular symbols indicate remarkably shorter bunches; this is our most recent data and we are presently performing a more comprehensive study of operation near these settings.

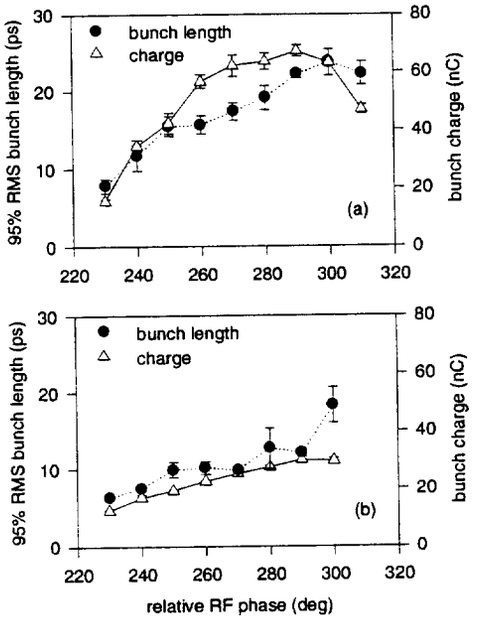

Figure 2: Bunch length and charge as a function of the RF phase: (a) high charge case; (b) low charge case. The error bars represent the standard deviation calculated by averaging three shots.

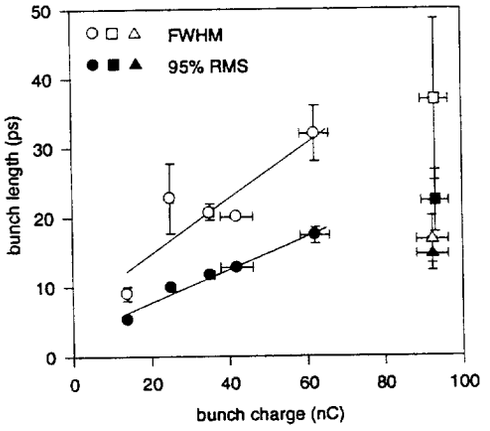

Figure 3: Measurements of electron bunch length as a function of bunch charge. The points represented by circles correspond to the average of three pulses. The squares and triangles correspond to the average of ten and sixteen pulses, respectively.

Emittance measurements of high charge electron beams are quite difficult. We attempted to measure the emittance of the drive beam with a pepper-pot plate. Unfortunately, the resulting images are rather irregular. We are now trying to determine if that is caused by scattering on the holes, by nonlinear response of the phosphor screen, or simply by a very irregular distribution of particles in the phase space.

We have measured the normalized emittance of the witness beam by quadrupole scan techniques (3.5 π mm mrad). This procedure could be applied to the drive beam, even with its high charge, since we have developed a quadrupole scan model that includes space-charge forces. However, our phosphor screens currently cannot withstand a focused 100 nC electron bunch.

4 DISCUSSION

We are approaching the design goals of the AWA facility (100 nC, 25 ps FWHM). There are still many aspects of the generation of these unprecedented high charge, short electron bunches that call for more detailed studies. While this constitutes an interesting and challenging research program in itself, we are concomitantly proceeding with experiments on plasmas and dielectric wakefields [4,5].

5 ACKNOWLEDGMENTS

We would like to thank L. Balka, A. Caired, C. Keyser, R. Taylor and K. Wood for their technical support.

This work is supported by the Department of Energy, Division of High Energy Physics, under contract No. W-31-109-ENG-38.

REFERENCES

[1] P. Schoessow et al., "The Argonne Wakefield Accelerator High Current Photocathode Gun and Drive Linac", Proc. 1995 Particle Accelerator Conf., pp. 976 - 978.

[2] J. Power et al., "Measurements of the Argonne Wakefield Accelerator's Low Charge, 4 MeV RF Photocathode Witness Beam", Proc. 1996 Advanced Accelerator Concepts Workshop.

[3] We thank J. Rosenzweig for initiating us in the use of aerogel radiators, and J. Oyang and P. Tsou for making them available to us.

[4] P. Schoessow et al., "High Gradient Dielectric Wakefield Device Measurements at the Argonne Wakefield Accelerator", These Proceedings.

[5] N. Barov et al., "Results of Blowout Regime Propagation of an Electron Beam in a Plasma", These Proceedings.